Synthesis, Characterization, and Crystal Structure of Dicalcium Glutarylbis(phosphonate) Dihydrate: A Covalently Pillared Layer Structure with the Potential for Epitaxial Growth on Hydroxyapatite

Mathai Mathew,*,† Bruce O. Fowler,‡ Eli Breuer,§ Gershon Golomb,|| Ivan S. Alferiev,⊥ and Naomi Eidelman†

Paffenbarger Research Center, American Dental Association Health Foundation, National Institute of Standards and Technology, Gaithersburg, Maryland 20899, National Institute of Dental Research's Craniofacial and Skeletal Diseases Branch Research Associate Program at the National Institute of Standards and Technology, Gaithersburg, Maryland 20899, Department of Pharmaceutical Chemistry, School of Pharmacy, The Hebrew University of Jerusalem, Jerusalem, Israel, Department of Pharmaceutics, School of Pharmacy, The Hebrew University of Jerusalem, Jerusalem, Israel, and Department of Pediatrics, School of Medicine, University of Pennsylvania, Philadelphia, Pennsylvania 19104

Received April 3, 1998

A new bis(acylphosphonate), glutarylbis(phosphonate) (GlBP), was synthesized. Sodium and calcium salts of the GlBP, disodium dihydrogen glutarylbis(phosphonate), $NaHO_3PC(O)(CH_2)_3C(O)PO_3HNa$, and dicalcium glutarylbis(phosphonate) dihydrate, $Ca_2[O_3PC(O)(CH_2)_3C(O)PO_3]\cdot 2H_2O$, were prepared and characterized by chemical analyses, thermogravimetry and Fourier transform infrared spectroscopy (FTIR). The crystal structure of the Ca salt was determined by single-crystal X-ray diffraction. The crystals are orthorhombic with $a = 10.970(1)$ Å, $b = 23.694(2)$ Å, $c = 5.580(1)$ Å, space group *Pnma*, and $Z = 4$. This study provides the first example of a structure of a calcium complex involving a nongeminal bis(phosphonate). The structure can be described in terms of a covalently pillared layer-type arrangement of neutral Ca−GlBP−Ca units along the *b*-axis. Each oxygen atom of the phosphonate group is bonded to a different Ca ion, and each Ca in turn is linked to three phosphonate groups. The Ca octahedra and the phosphonate tetrahedra form a two-dimensional polar sheet perpendicular to the *b*-axis. The chelate bonds involving the keto groups appear to be important links in the stabilization of the structure and, in turn, to the biological activity of bis(acylphosphonates). A near-perfect lattice match, found between the Ca phosphonate layer and the major crystal faces of hydroxyapatite, indicates that epitaxial growth or incorporation of GlBP can occur on the apatitic surface which may be the mode of action in the inhibition of calcification.

Introduction

Bis(phosphonates) (BPs) are a class of drugs which have been developed for diagnostic and therapeutic use in various diseases of bone and calcium metabolism.[1−7] Until recently, most of the research in this field has been confined to geminal bis(phosphonates) (compounds of the general structure P−C−P; see Figure 1), with various modifications of the side chains attached to the central carbon atom (X, Y in Figure 1). In contrast to the geminal bis(phosphonates), monophosphonates and longer chain bis(phosphonates) (of the type $P-C_n-P$ with $n \geq 2$; Figure 1) have been reported to be inactive with respect to calcium-related disorders.[2,3] Recently however, nongeminal bis(phosphonates) with keto groups at α positions relative to the phosphonate groups (of the type $O_3P-C(=O)(CH_2)_nC(=O)PO_3$, termed bis(acylphosphonates); Figure 1) have been reported to be active as anticalcification and antiresorption agents.[8−10] The bis(acylphosphonates) with shorter hydrocarbon chains ($n = 3-6$) showed stronger activity in the *in vitro*[10] and *in vivo*[8,9] studies. They apparently possess lower toxicity, and their calcium complexes have improved solubility properties and, therefore, are of potential importance in clinical applications.[9,10]

Although the precise mechanisms of action of BPs are not yet known, some of the biological effects of geminal bis(phosphonates) have been attributed to their physicochemical

* Corresponding author. Fax: 301-963-9143. E-mail: mathai.mathew@nist.gov.
† Paffenbarger Research Center, NIST.
‡ National Institute of Dental Research's Craniofacial and Skeletal Diseases Branch Research Associate Program at NIST.
§ Department of Pharmaceutical Chemistry, The Hebrew University of Jerusalem.
|| Department of Pharmaceutics, The Hebrew University of Jerusalem.
⊥ University of Pennsylvania.

(1) Fleisch, H. *Drugs* **1991**, *42*, 919.
(2) Francis, M. D.; Martodam, R. R. In *The Role of Phosphonates in Living Systems*; Hilderbrand, R. L., Ed.; CRC Press: Boca Raton, FL, 1983; p 55.
(3) Fleisch, H. *Bone* **1987**, *8*, S23.
(4) Schoen, F. J.; Harasaki, H.; Kim, K. M.; Anderson, H. C.; Levy, R. J. *J. Biomed. Mater. Res.* **1988**, *22*, 11.
(5) Rubin, R. P.; Weiss, G. B.; Putney, J. W., Jr. *Calcium in Biological Systems*; Plenum Press: New York, 1985.
(6) Fleisch, H. *Bisphosphonates in Bone Disease. From the Laboratory to the Patient*, 2nd ed.; The Parthenon Publishing Group: New York, 1995.
(7) Mundy, G. R. *Bone* **1987**, *8*, S9.
(8) Golomb, G.; Schlossman, A.; Saadeh, H.; Levi, M.; Van Gelder, J. M.; Breuer, E. *Pharm. Res.* **1992**, *9*, 143.
(9) van Gelder, J. M.; Breuer, E.; Ornoy, A.; Schlossman, A.; Patlas, N.; Golomb, G. *Bone* **1995**, *16*, 511.
(10) Skrtic, D.; Eidelman, N.; Golomb, G.; Breuer, E.; Eanes, E. D. *Calcif. Tissue Int.* **1996**, *58*, 347.

10.1021/ic980374h CCC: $15.00
Published on Web 11/20/1998

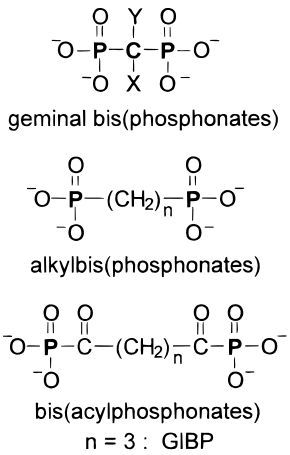

Figure 1. General structures of geminal bis(phosphonates), alkylbis(phosphonates) and bis(acylphosphonates).

interactions with calcium phosphate crystals, either through adsorption, incorporation, or epitaxial growth.[2,3] An examination of Ca/bis(phosphonate) complex formation under physiological conditions and structural studies of the complexes may provide a basis for the mode of action of these phosphonates in controlling Ca-related disorders. Knowing the mode of interaction of biologically active BPs with calcium may lead to an understanding of the mechanism of action of these drugs and may help in the rational design of new improved analogues.

Despite the large number of bis(phosphonates) investigated for biological activity, or even used clinically, structural studies of calcium complexes of BPs are very limited. Only two such studies exist: one on (1-hydroxyethylidene)bis(phosphonate) (HEBP),[11] another on (dichloromethylene)bis(phosphonate) (ClMBP).[12] Both studies involve partially ionized geminal BPs, CaH_2HEBP[11] and CaH_2ClMBP.[12] A common feature in these structures is that the Ca ion forms a six-membered chelate ring with two terminal phosphonyl oxygens. However, this mode of linking cannot be expected in nongeminal BPs. The presence of a potential donor group adjacent to the phosphonate group in the monophosphonates, sodium acetylphosphonate[13] and calcium (α-hydroxyimino)phosphonate,[14] has been found to form bidentate chelates with the metal ions. The bis(acylphosphonates) would be expected to behave in a similar fashion. As part of a program to investigate the validity of this concept, and to correlate the possible effects of the chelation on the biological activity, structural studies of various calcium bis(acylphosphonates) were undertaken. We have synthesized a new bis(acylphosphonate), disodium dihydrogen glutarylbis(phosphonate), $NaHO_3PC(O)(CH_2)_3C(O)PO_3HNa$ (Na_2H_2GlBP), and were able to prepare single crystals of a calcium salt of the completely ionized GlBP (Figure 1) at physiological pH. The crystal structure of this compound, dicalcium glutarylbis(phosphonate) dihydrate, $Ca_2[O_3PC(O)(CH_2)_3C(O)PO_3]\cdot 2H_2O$ (CaGlBPD), is reported here. This study provides the first example of a structure of a calcium complex involving a nongeminal bis(phosphonate).

Experimental Section[51]

Preparation of Disodium Dihydrogen Glutarylbis(phosphonate). A solution of glutaryl chloride (5.0 mmol) in dry tetrahydrofuran (THF) (10 mL) was cooled to −50 °C in an argon atmosphere. Tris(trimethylsilyl) phosphite (3.34 mL, 10.0 mmol) was added dropwise under vigorous stirring at the temperature range, −50 to −55 °C within 15 min. The mixture was stirred within these temperatures for an additional 1.5 h, and then methanol (10 mL) was introduced with the temperature increasing from −50 to −25 °C. The mixture was stabilized by pouring it into a cold (−50 °C) solution of triethylamine (5 mL) in methanol (20 mL). Volatile products were removed completely in vacuo (at temperatures below 30 °C), and the resulting syrup was diluted with methanol (25 mL) to give a relatively stable solution of triethylammonium salts. The latter could be stored at 0−10 °C over a period of at least 1 month without any noticeable change in ^{31}P NMR spectrum.

Analysis of the reaction solutions by ^{31}P NMR showed that the signals corresponding to $C(O)-PO_3H_2$ groups (0 ppm) were found to amount to about 78% of total ^{31}P signals. The triethylamine methanol solution was concentrated in vacuo (at temperature below 35 °C) to a syrup, dissolved in methanol (4 mL), and mixed with a solution of piperazine hexahydrate (2.65 g, 13.6 mmol) in methanol (9.6 mL) and water (10.9 mL) with acetic acid (2.18 mL, 38.2 mmol). Crystallization began immediately. After standing overnight, the precipitate was filtered off, washed with a mixture of methanol (7 mL) and water (3 mL) and washed again with methanol, and then air-dried to give a yield of 1.33 g of pure glutarylbis(phosphonate) dipiperazine heptahydrate salt (mass fraction = 48% of the theoretical value) according to ^{31}P NMR (the only singlet was at −0.5 ppm in water adjusted to pH = 7 with $NaHCO_3$).

The elemental analyses of glutarylbis(phosphonate) dipiperazine heptahydrate and Na_2H_2GlBP were performed by the Analytical Laboratories of the Hebrew University of Jerusalem (Givat Ram, Jerusalem, Israel). Nuclear magnetic resonance spectra were obtained with Varian VXR-300S (Palo Alto, CA) or Bruker-WH-300S (Bruker, Rheinstetter, Germany) spectrometers. ^1H NMR and ^{31}P NMR spectra were recorded in deuteriochloroform or in deuterium oxide solutions. Chemical shifts are reported as parts per million from tetramethylsilane (TMS) as the internal standard for ^1H NMR and from H_3PO_4 (mass fraction = 10%) as the external standard for ^{31}P NMR; positive chemical shifts are at low field with respect to the standards.

Analyses are as follows. Anal. Calcd for $C_{13}H_{30}N_4O_8P_2\cdot 7H_2O$: C, 27.96; H, 7.94; N, 10.03: P, 11.09. Found: C, 27.76; H, 6.40; N, 9.90; P, 11.50. NMR: ^1H (D_2O, immediately after dissolution), δ, ppm, 1.75 (quint, 6 Hz, 2H, β-CH_2), 2.81 (t, 6 Hz, 4H, CH_2CO), 3.42 (s, 16H, piperazine); ^{31}P NMR (D_2O, immediately after dissolution), −0.7 ppm, s.

The glutarylbis(phosphonate) dipiperazine heptahydrate is stable for at least 2 months at room temperature when stored in the dark. In aqueous solutions (especially at a lower pH in the presence of Na cations) additional peaks in ^{31}P NMR may appear in the regions ca. 5 and ca. 14 ppm, probably due to cyclization. The glutarylbis(phosphonate) dipiperazine salt can easily be transformed into the disodium salt as described below.

Glutarylbis(phosphonate) dipiperazine heptahydrate salt (4.76 g, 8.52 mmol) was dissolved in water (100 mL) and passed through Dowex-50 cation-exchange resin (H^+ form, eluted with water until neutral). The pH of the eluate (200 mL) was adjusted with a solution of sodium hydroxide to pH = 4. The solution was concentrated in vacuo to a syrupy mass (3.0 g), which was diluted with methanol (20 mL) and allowed to stand for 1 h.

(11) Uchtman, V. A. *J. Phys. Chem.* **1972**, *76*, 1304.
(12) Nardelli, M.; Pelizzi, G.; Staibano, G.; Zucchi, E. *Inorg. Chim. Acta* **1983**, *80*, 259.
(13) Jones, P. G.; Kennard, O. *Acta Crystallogr.* **1978**, *B34*, 2309.
(14) Gibson, D.; Karaman, R. *J. Chem. Soc., Dalton Trans.* **1989**, 1911.

The precipitate was filtered off, washed with methanol, and air-dried; the yield was 2.58 g (mass fraction = 99%) of anhydrous NaH_2GlBP.

Analyses are as follows. Anal. Calcd for $C_5H_8O_8P_2Na_2$: C, 19.75; H, 2.65; P, 20.37. Found: C, 19.63; H, 2.56; P, 19.94. NMR: ^{1}H NMR ($D_2O + Na_2CO_3$, pH = 8, immediately after dissolution), δ, ppm, 1.73 (quint., 7 Hz, 2H, β-CH_2), 2.82 (t, 7 Hz, 4H, CH_2CO); ^{31}P NMR ($D_2O + Na_2CO_3$, pH = 8), −0.2 ppm, s.

Preparation of Dicalcium Glutarylbis(phosphonate) Dihydrate Single Crystals. Single crystals were prepared by gel-diffusion methods. Single crystals of CaGlBPD were grown in U tubes in gelatin gel (7% mass fraction gelatin, pH = 5.8) relatively easily at room temperature (23 °C) in about 2−3 weeks, but they were too small for single-crystal studies. Larger crystals, suitable for X-ray structure analysis, were grown in silica gel at 32 °C and pH = 7.35. Initially, an aqueous solution of Na_2H_2GlBP (10 mL, 100 mmol/L, pH = 7.0) was placed on the silica gel in one arm of a U tube and an aqueous solution of $Ca(NO_3)_2$ (10 mL, 200 mmol/L, pH = 7.0) was placed in the other arm, all at room temperature. When there was no appreciable crystal growth even after 2 months at this temperature, the U tube was placed in an oven at 32 °C. Thin rectangular plates (0.2−0.5 mm width, several mm long, and 0.02−0.06 mm thick) formed at the bottom of the U tube after an additional 2 months. The crystals were retrieved from the gel, washed with distilled water, and air-dried.

Crystals from the gelatin gel preparation were analyzed by FTIR spectroscopy, powder X-ray diffraction (PXRD), thermogravimetric analysis (TG), and chemical analyses for C, H, P, and Ca. Crystals from the silica gel preparation were analyzed by FTIR and PXRD and for Ca content only because of the small yield. FTIR spectra were obtained from 256 coadded scans at 2 cm^{-1} resolution with a Nicolet Magna-IR 550 FTIR spectrometer continuously purged with dry air. Spectra of the crystals (0.8 mg, ground to ≤ 10 μm particle size) suspended in KBr pellets (400 mg, 13 mm diameter, ~1 mm thick) were recorded in the 4000−400 cm^{-1} region. TG was performed with a Perkin-Elmer 7 series thermal analysis system, in the temperature range from 30 to 800 °C at a rate of 10 °C/min in a nitrogen atmosphere. Samples were also heated at 180 °C in air for 18 h to effect dehydration, and then the mass loss was determined. PXRD patterns of the ground crystals (≤ 10 μm) were recorded with a Rigaku Dmax-2200 diffractometer, Cu Kα_1, λ = 1.540 56 Å. The standard uncertainty of measuring the d spacing values was ≤ 0.0013 Å, and the measured d values were within 0.05% of the reported values of NIST SRM 640 (silicon powder, 2θ = 28.442, d = 3.1355). Chemical analyses for C, H, P, and Ca on crystals from the gelatin preparation were done by Galbraith Laboratories, Knoxville, TN. The relative standard deviation for C determination was 0.5%; for H, 1.3%; for P, 4.5%; and for Ca, 3.4% (the uncertainty is not available on these non-NIST data). Ca analysis on single crystals from the silica gel preparation was determined by atomic absorption with a Perkin-Elmer 603 spectrophotometer. The standard uncertainty was 0.05.

A single crystal grown from silica gel and cut to a suitable size (0.30 × 0.24 × 0.04 mm) was used for data collection. Diffraction data was collected on an Enraf-Nonius CAD-4 diffractometer with graphite-monochromatized Mo Kα radiation. The structure was solved by direct methods and refined by the full-matrix least-squares method. Details of crystallographic parameters are given in Table 1.

Table 1. Crystallographic Data for Dicalcium Glutarylbis(phosphonate) Dihydrate

formula	$Ca_2(P_2O_8C_5H_6)0{\cdot}2H_2O$
fw	372.24
space group	*Pnma* (No. 62)
temp	20 °C
a	10.970(1) Å
b	23.694(2) Å
c	5.580(1) Å
V	1450.3(3) Å^3
Z	4
ρ_{calc}	1.704 g cm^{-3}
ρ_{meas}	1.71 g cm^{-3}
μ	10.1 cm^{-1}
$R(F_o)^a$	0.023
$R_w(F_o)^b$	0.044

^{a} $R = \sum(|F_o| - |F_c|)/\sum|F_o|$. ^{b} $R_w = [\sum w(|F_o| - |F_c|)^2/\sum w|F_o|^2]^{1/2}$, $w = 1/(\sigma(F_o)^2 + 0.0004F_o^2)$.

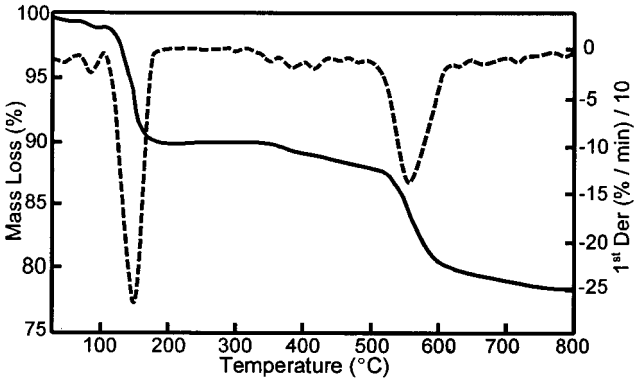

Figure 2. TG mass loss (solid line) and first derivative (dashed line) curves for CaGlBPD prepared in gelatin gel.

Results

Synthesis and Characterization. Unlike adipoyl or longer chain dicarboxylic acid dichlorides, which produced only the corresponding bis(acylphosphonates) in the Arbuzov reaction with trimethyl phosphite,[8,9] the reaction of glutaryl chloride with trimethyl phosphite gave complex mixtures from which the isolation of the desired product was not practical. Therefore, the synthesis of glutarylbis(phosphonate) required a different approach. We succeeded in synthesizing this compound by reacting glutaryl chloride with tris(trimethylsilyl) phosphite. The tetrakis(trimethylsilyl) glutarylbis(phosphonate) thus obtained was alcoholyzed by methanol to glutarylbis(phosphonic acid), which could be precipitated in pure form from the reaction mixture as the piperazine salt. Piperazine salts were shown to be suitable for isolation of glutaryl-, pimeloyl-, and suberoylbis-(phosphonates). They are not hygroscopic and can be purified to analytical grade by reprecipitation from aqueous solutions by addition of methanol. The piperazine salts could easily be converted to disodium salts after treatment with a cation-exchange resin.

The chemical analyses for CaGlBPD were the following. Calcd for $C_5H_{10}O_{10}P_2Ca_2$: C, 16.13; H, 2.71; P, 16.64; Ca, 21.54. Found for sample prepared in gelatin gel: C, 16.6; H, 2.88; P, 18.1, Ca, 24.18. The Ca/P molar ratio was 1.007 vs the calculated 1.0. The mass fraction % of Ca in CaGlBPD prepared in silica gel was 21.48%.

The TG mass loss curve and its first derivative curve for CaGlBPD prepared in gelatin gel are shown in Figure 2. The loss of hydrated water in CaGlBPD started at around 120 °C and was completed around 180 °C; no additional weight loss occurred until about 340 °C. The observed weight loss of 8.93%

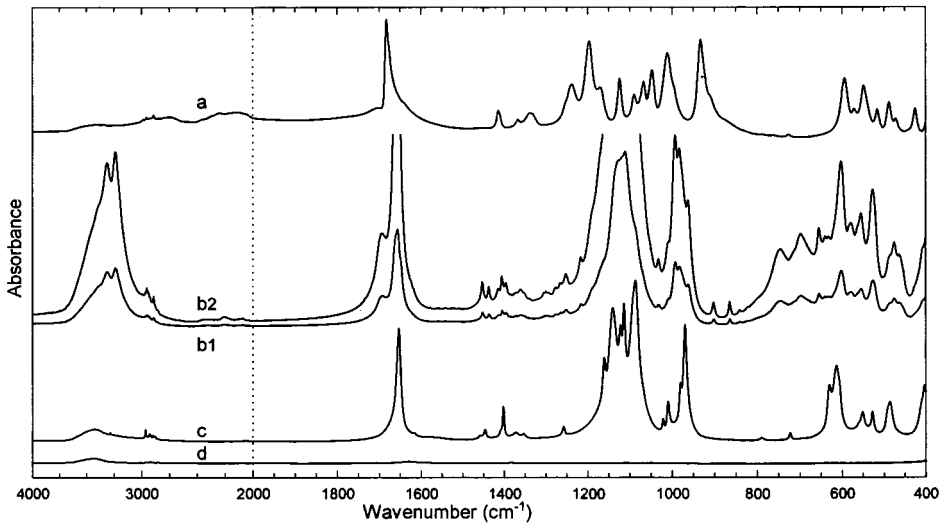

Figure 3. Infrared spectra of (a) Na_2H_2GlBP, (b1) CaGlBPD prepared in gelatin gel, (b2) absorbance expansion of (b1), (c) CaGlBPD prepared in gelatin gel heated at 180 °C in air for 18 h to form anhydrous CaGlBP, and (d) the baseline from a blank KBr pellet.

between 120 and 180 °C is in reasonable agreement with the calculated value of 9.68% for the removal of two water molecules. The relative mass losses of 2.6% between ~340 and 530 °C, 7.1% between ~ 530 and 590 °C, and 2.0% between ~590 and 800 °C probably correspond to the decomposition of the keto and the CH_2 groups; however, no study was carried out to identify with clarity the decomposition products at the higher temperatures. The two samples of CaGlBPD that were heated at 180 °C in air for 18 h had a relative mass loss of 9.35 ± 0.08%.

FTIR spectra of Na_2H_2GlBP, CaGlBPD, and anhydrous CaGlBPD samples are shown in Figure 3. The spectra from the gelatin and silica gel preparations were practically identical except for two impurity bands apparently from the silica gel matrix in the silica gel preparation (band at 1569 cm^{-1} and broad band at ~1470−1350 cm^{-1}). The spectrum of anhydrous CaGlBP (formed by heating CaGlBPD at 180 °C in air for 18 h) was used to aid in assignments of water molecules in the hydrated CaGlBPD. The wavenumbers (cm^{-1}) and infrared band assignments for CaGlBPD (gelatin gel preparation) are summarized in Table 2. The cm^{-1} positions of bands were obtained from second derivatives of spectra, and some of the bands listed in Table 2 are not obvious in the condensed spectra shown in Figure 3. The accuracy was $<\pm$ 0.01 cm^{-1} according to the Nicolet spectrometer specification; the cm^{-1} were rounded off to the nearest 1 cm^{-1}. The main characteristic infrared bands of the PO_3 group occur in three regions: ~1120, ~980, and 600−460 cm^{-1}. The characteristic infrared bands of the α-keto group (C═O) occur at ~1660 cm^{-1}, and the main bands of the water molecules are at 3312, 3236, 1696, 746, and 698 cm^{-1}.

The PXRD patterns of the two samples of CaGlBPD, prepared in both gelatin gel and silica gel, were practically identical. The observed *d* spacings obtained from the PXRD pattern of the gelatin gel preparation and *d* spacings and corresponding intensities, both calculated from the single-crystal data obtained from a crystal from the silica gel preparation, along with *hkl* values, are given in Table 3. The average difference between the observed and calculated *d* spacing value was 0.10%.

Although the single crystals from the silica gel preparation used for the structure determination were not analyzed for C, H, and P or by TG because of the small yield, the combined IR, PXRD, and Ca data indicate, except for the minor impurity in the bulk ground crystals from the silica gel preparation, that the crystals from the gelatin gel and silica gel preparations are the same.

Table 2. Wavenumbers (cm^{-1}) and Infrared Band Assignments for CaGlBPD[a]

band (cm^{-1})	assignments
3312 m	ν_3 stretch of H-bonded H_2O
3236 m	ν_1 stretch of H-bonded H_2O
2990 vw, 2975 vw, 2965 vw, 2952 w, 2938 vw, 2922 vw	CH_2 antisymmetric stretch
2903 vw, 2891 w, 2853 vw	CH_2 symmetric stretch
~2400 vw	?
~2257 vw	overtones of PO_3 stretch
~2089 vw	combinations of PO_3 stretch
1696 w	ν_2 bend of H-bonded H_2O
1662 s, 1656 s, 1648 s	C═O stretch
1452 w, 1436 w, 1414 w, 1405 w	CH_2 bend
1395 w, 1384 vw, 1374 vw, 1361 w	CH_2 wag
1350 vw, 1338 vw, 1305 vw, 1299 vw, 1292 vw, 1277 vw, 1266 vw, 1252 w, 1216 vw, ~1192 vw, ~1170 vw	CH_2 wag or CH_2 twist
~1137 sh, 1129 vs, 1120 vs, 1111 vs, ~1087 m	PO_3 antisymmetric stretch
1032 w, 1010 w	CC stretch
993 m, 982 m, 974 sh, 961 m	PO_3 symmetric stretch
902 w, 864 w, 841 vw	CC stretch or CH_2 rock
746 m, 698 m	H_2O libration
655 m	?
640 vw, 632 vw	CO bend?
602 m	PO_3 bend
578 w	?
554 m, 527 m, ~488 m, 475 m	PO_3 bend
463 w	CO bend?

[a] s, strong; m, medium; w, weak; v, very; sh, shoulder.

Crystal Structure. The final atomic parameters of CaGlBPD are listed in Table 4; selected bond lengths and bond angles are listed in Table 5. The atomic numbering scheme is shown in Figure 4, and the molecular packing is illustrated in Figure 5.

The crystal structure can be described in terms of a layer-type arrangement of neutral Ca−GlBP−Ca chains stacked along the *b*-axis. The calcium atom is coordinated to six oxygen atoms, four from four different phosphonate groups, one from a keto group, and one from a water molecule. The Ca−O distances are in the range 2.276(2)−2.438(2) Å. There are no other Ca−O

Table 3. Observed and Calculated XRD Patterns for CaGlBPD[a]

h	*k*	*l*	d_o	d_c	I_c
0	2	0	11.820	11.847	100.0
0	4	0	5.913	5.924	5.8
2	0	0		5.485	3.7
0	1	1	5.425	5.431	6.4
2	1	0	5.338	5.344	10.9
2	2	0		4.977	1.5
1	0	1	4.967	4.974	12.1
1	2	1	4.579	4.586	3.3
1	3	1	4.205	4.209	1.5
2	4	0	4.014	4.025	0.3
0	6	0	3.942	3.949	11.3
2	0	1	3.906	3.912	11.5
2	3	1	3.501	3.505	1.7
1	6	1	3.089	3.093	2.3
3	0	1	3.052	3.059	2.0
3	1	1	3.029	3.033	6.8
2	5	1	3.016	3.017	3.6
0	8	0	2.957	2.962	5.3
3	2	1		2.961	1.6
3	3	1	2.849	2.852	10.0
1	7	1	2.795	2.798	1.6
1	0	2	2.700	2.704	0.9
1	1	2	2.683	2.687	1.5
1	2	2	2.634	2.636	1.4
3	5	1		2.570	1.8
1	3	2	2.555	2.558	1.8
1	8	1	2.542	2.545	4.9
4	0	1	2.459	2.461	1.1
3	6	1	2.411	2.418	1.1
0	9	1	2.377	2.381	0.8
4	5	0		2.374	1.1
0	10	0	2.367	2.369	0.9
1	9	1	2.345	2.327	1.1
2	9	1	2.181	2.184	1.7
2	10	0	2.174	2.175	2.2
3	3	2		2.136	1.6
3	8	1	2.128	2.128	1.3
5	1	1	2.032	2.034	0.2
1	8	2	1.994	1.997	2.1
4	3	2	1.897	1.899	0.7
2	11	1	1.885	1.887	0.7
4	5	2	1.807	1.808	0.8
6	3	0	1.780	1.781	1.5
3	8	2	1.776	1.775	0.1
2	12	1	1.759	1.763	0.0
2	3	3	1.718	1.719	0.8
6	5	0	1.705	1.706	1.5
0	14	0	1.690	1.692	0.6
5	3	2	1.684	1.685	1.6
2	5	3	1.650	1.651	1.6
1	14	1	1.601	1.602	0.7

[a] The observed *d* values (d_o) are for the sample prepared in gelatin gel. The calculated *d* values (d_c) and intensities (I_c) are based on the single crystal parameters.

contacts less than 3.2 Å to indicate any additional coordination of Ca. The coordination around Ca corresponds to a slightly distorted octahedron with three phosphonate O atoms and one water molecule in the equatorial plane (Figure 5). The Ca octahedra share one corner through O(3) from an adjacent Ca phosphonate layer.

The keto oxygen and one of the phosphonyl oxygens form a bidentate chelate bond to the Ca ion. However, each oxygen atom of the phosphonate group is linked to a different Ca ion and each Ca ion, in turn, is linked to different phosphonate groups (Figure 5). The metal phosphonate coordination ratio is 4:4. The Ca octahedra and the phosphonate tetrahedra form an infinite two-dimensional polar sheet perpendicular to the *b*-axis. All the Ca ions in this sheet are exactly planar with the hydrocarbon chains perpendicular to the Ca plane (Figure 4).

Table 4. Final Atomic Parameters in CaGlBPD

atom	*x*	*y*	*z*	B_{eq}[a]
Ca	0.20816(4)	0.05888(2)	0.58153(9)	1.11(1)
P	0.39846(5)	0.07450(3)	0.09653(11)	1.03(1)
O1	0.5336(2)	0.07167(8)	0.1430(3)	1.55(3)
O2	0.3679(2)	0.07483(8)	−0.1673(4)	1.85(4)
O3	0.3229(2)	0.03208(7)	0.2378(4)	1.56(3)
O4	0.2803(2)	0.14510(8)	0.3899(4)	2.18(4)
Ow	0.0859(2)	0.1002(1)	0.8850(3)	2.57(4)
C1	0.3491(2)	0.1436(1)	0.2175(5)	1.65(5)
C2	0.3949(3	0.1968(1)	0.1016(6)	3.75(7)
C3	0.3512(5)	0.2500[b]	0.2227(5)	3.8(1)
Hw1	0.026(3)	0.095(1)	0.842(6)	4.6(8)[c]
Hw2	0.076(3)	0.085(1)	0.031(7)	4.3(8)[c]
H2a	0.491(4)	0.193(2)	0.077(6)	6(1)[c]
H2b	0.375(3)	0.191(1)	0.930(7)	5(1)[c]
H3a	0.265(5)	0.250	0.190(11)	7(2)[c]
H3b	0.392(5)	0.250	0.402(10)	6(1)[c]

[a] $B_{eq} = (4/3)\sum\sum_{ij}\beta_{ij}a_i \cdot a_j$. [b] Parameters without standard deviations are fixed by symmetry. [c] Hydrogen atoms were refined with isotropic thermal parameters.

Table 5. Bond Lengths (Å) and Angles (deg) in CaGlBPD[a]

Ca−O2	2.276(2)	P−O1	1.507(2)
Ca−O1	2.308(2)	P−O2	1.510(2)
Ca−O3[i]	2.350(2)	P−O3	1.523(2)
Ca−Ow	2.372(2)	P−C1	1.853(3)
Ca−O3	2.380(2)	C1−O4	1.223(3)
Ca−O4	2.438(2)	C1−C2	1.503(4)
		C2−C3	1.508(4)
O1−P−O2	112.7(1)	P−C1−C2	119.1(2)
O1−P−O3	114.7(1)	P−C1−O4	119.5(2)
O2−P−O3	112.8(1)	C2−C1−O4	121.4(2)
C1−P−O1	105.3(1)	C1−C2−C3	113.7(3)
C1−P−O2	106.6(1)	C2−C3−C2[ii]	113.3(3)
C1−P−O3	103.6(1)		

Probable Hydrogen Bond Parameters Involving Water Molecules

D−H···A[b]	D−H	H···A	D−A	D−H−A
Ow−Hw1−O2	0.71(3)	2.05(3)	2.749(3)	170(4)
Ow−Hw2−O1	0.89(4)	1.91(4)	2.779(2)	165(3)

[a] Symmetry codes: (i) $^1/_2 - x, -y, ^1/_2 + z$; (ii) $x, ^1/_2 - y, z$. [b] Donor−hydrogen···acceptor.

The GlBP ion is on a crystallographic mirror plane perpendicular to the hydrocarbon chain, through the central carbon atom, C3. Thus, each bis(phosphonate) ion is linked to six Ca ions in two polar sheets with the hydrocarbon chain sandwiched between these sheets. The Ca−bis(phosphonate)−Ca chains are stacked parallel to the *b*-axis, and the stacks are packed along the *b*-axis (Figure 5). The arrangement results in a layer-type structure with the sequence ABAABA..., where A corresponds to the polar Ca phosphonate layer and B to the hydrophobic hydrocarbon layer. The only linkage between adjacent AA layers along the *b*-axis is a corner sharing of a Ca octahedra.

Discussion

Chemical Composition. The chemical analyses for Ca, H, C, and P are consistent with the calculated values of the compositional formula of $Ca_2[O_3PC(O)(CH_2)_3C(O)PO_3]\cdot 2H_2O$, and the TG results agree reasonably well with the presence of two water molecules in the structure. The FTIR spectra identified and confirmed the presence of PO_3, C═O, CH_2 functional groups, and H_2O molecules in the crystals.

Infrared Spectra. The bis(acylphosphonate) ion (GlBP, Figure 1), $O_3PC(O)(CH_2)_3C(O)PO_3$, has C_s site symmetry in CaGlBPD; the ion has a crystallographic mirror plane perpendicular to the hydrocarbon chain, through the central atom, C3

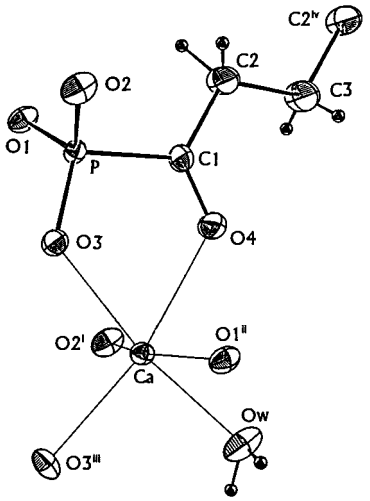

Figure 4. Molecular structure of CaGlBPD showing the atomic numbering scheme. Only the asymmetric part of the molecule is shown. The non-hydrogen atoms are shown as 50% ellipsoids, and the H atoms are depicted as spheres with $B = 1.5$ Å^2.

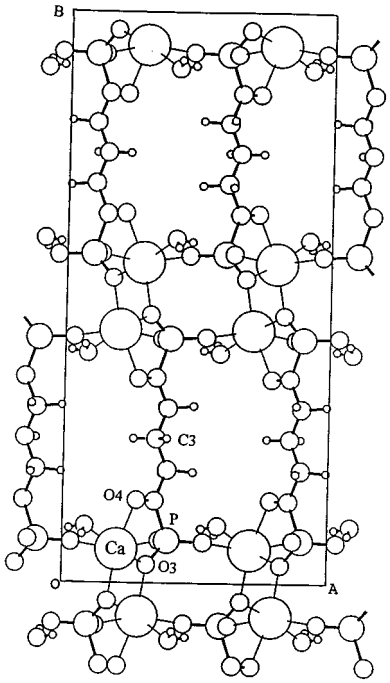

Figure 5. Packing diagram showing the unit cell and the layered structure for CaGlBPD.

(Figure 5). According to the C_s point group for the 21 atom GlBP ion, 57 internal vibrational modes distributed among A′ and A″ species, all both IR and Raman active, are predicted. In addition, more than 57 bands can occur due to factor group coupling between the 57 modes of each of the 4 equivalent GlBP ions in the unit cell. In the present study, only characteristic type assignments are given for the functional groups PO_3, C═O, and CH_2 of the GlBP ion. The vibrational modes and wavenumber positions of the C═O and CH_2 groups[15,16] are well-known and the symmetric and antisymmetric stretching modes of the PO_3 groups have been characterized,[17,18] but very little work has been reported on the PO_3 bending modes.

PO_3 Bands. The highest symmetry for the isolated pyramidal PO_3 group is C_{3v}; this C_{3v} point group gives rise to four modes[19] composed of 2E and $2A_1$ modes. The crystal structure analysis (Table 5) shows that the PO_3 group has C_1 symmetry from its unequal bond lengths and angles; consequently, the degeneracies are removed and the four 2E and $2A_1$ modes become 6 modes composed of 3 stretching and 3 bending modes. Since the GlBP ion has two equivalent PO_3 groups separated by a mirror plane in the chain, each of the 3 stretching and 3 bending modes is expected to be split with a resultant total of 6 stretching and 6 bending modes. The groups of strong-intensity bands at 1137, 1129, 1120, 1111, and 1087 cm^{-1} are assigned to antisymmetric stretching modes of the PO_3 ions, and the groups of medium-intensity bands at 993, 982, 974, and 961 cm^{-1} are assigned to symmetric stretching modes of the PO_3 ions. Tsuboi[18] and Shimanouchi et al.[20] have given assignments for the stretching and bending modes of PO_3 groups; their assignments for the PO_3 bending modes of solid $BaHPO_3$ are at 591, 498, and 471 cm^{-1}. Consequently, the GlBP bands at 602, 554, 527, 488, and 475 cm^{-1} are assigned to bending modes of the PO_3 groups.

C═O Bands. Two or more C═O stretching bands are expected in the 1700 cm^{-1} region, and four or more C═O bending bands of the 2 [P−C(O)−C] groups are expected in the region from about 600−400 cm^{-1}. The bands at 1662, 1656, and 1648 cm^{-1} are assigned to C═O stretching modes, but band assignments for the bending bands are uncertain. Previous normal coordinate calculations[21] of several aliphatic ketones place the C−C(O)−C in-plane bending and out-of-plane bending bands at 628−594 and 460−437 cm^{-1}, respectively. Since the bending modes of the PO_3 and C−C(O)−C groups occur in the same wavenumber region, no unambiguous assignments can be made with the present data, although the bands at 640, 632, and 463 cm^{-1} may derive from P−C(O)−C bending modes.

CH_2 Bands. Six or more CH_2 stretching bands, composed of three antisymmetric and three symmetric bands from the 3 (CH_2) groups, are expected. In the CH_2 stretching region, about 2990−2840 cm^{-1}, the six bands with wavenumbers higher than 2939 cm^{-1} are tentatively assigned to the antisymmetric CH_2 stretching modes, and the three bands with wavenumbers 2923 cm^{-1} and lower are tentatively assigned to the CH_2 symmetric stretching modes. Three or more CH_2 bending modes are expected in the region from about 1460−1400 cm^{-1}. The bending modes of CH_2 groups adjacent to C═O groups are well-known to occur in the 1435−1405 cm^{-1} region;[15] thus, the two bands at 1405 and 1414 cm^{-1} are assigned to bending bands of the two C(2)H_2 and C(2′)H_2 groups adjacent to the C═O groups and the band at 1452 cm^{-1} to CH_2 bending of the central C(3)-H_2 group. The fourth band in this region at 1436 cm^{-1} may arise from coupling between CH_2 bending modes. Three CH_2 wagging, three CH_2 twisting, and three CH_2 rocking bands are expected; however, more than three bands for each mode may occur due to coupling. The CH_2 wagging, twisting, and rocking

(15) Alpert, N. L.; Keiser, W. E.; Szymanski, H. A. *IR*: *Theory and Practice of Infrared Spectroscopy*, 2nd ed.; Plenum Press: New York, 1970; p 218.
(16) Socrates, G. *Infrared Characteristic Group Frequencies: Tables and Charts*, 2nd ed.; Wiley: Chichester, U.K., 1994; Chapters 2 and 10.
(17) Thomas, L. C. *Interpretation of the Infrared Spectra of Organophosphorus Compounds*; Heyden: London, 1974; p 165.
(18) Tsuboi, M. *J. Am. Chem. Soc.* **1957**, *79*, 1351.
(19) Herzberg, G. *Molecular Spectra and Molecular Structure. II. Infrared and Raman Spectra of Polyatomic Molecules*; D. Van Nostrand: Princeton, NJ, 1964; p 154.
(20) Shimanouchi, T.; Tsuboi, M.; Kyogoku, Y. In *Advances in Chemical Physics-Volume VII: The Structure and Properties of Biomolecules and Biological Systems*; Duchesne, J., Ed.; Interscience Publishers: London, 1964; Chapter 12.
(21) Shimanouchi, T.; Abe, Y.; Mikami, M. *Spectrochim. Acta* **1968**, *24A*, 1037.

modes in normal paraffins[22] and adipic acid[23] occur in the about 1410−1174, 1320−1170, and 1060−720 cm^{-1} regions, respectively. Fifteen weak intensity bands are observed in the CH_2 wagging and twisting region, about 1400−1170 cm^{-1}; these bands are grouped under CH_2 wag and CH_2 wag or twist assignments in Table 2.

H_2O Bands. The water molecules in $Ca_2GlBP{\cdot}2H_2O$ are located on C_1 symmetry sites. The free H_2O molecule has C_{2v} point group symmetry. For C_{2v} symmetry, the water molecule has nine vibrational modes composed of the following. (a) Three internal modes: ν_1, symmetric OH stretching; ν_2, symmetric OH bending; ν_3, antisymmetric OH stretching. (b) Six external modes: three librations and three translations.[24] On distortion to lower symmetry, C_s or C_1 from the site, all nine of these vibrations are both infrared and Raman active. There are eight water molecules in the unit cell, and all are on equivalent sites; if strong coupling occurs between modes of these equivalent molecules, the nine vibrational modes of each molecule can split into additional modes. The water librational bands[25] occur as high as 850 cm^{-1} and are present in our spectra whereas the translational bands normally occur[26] below about 300 cm^{-1} and are outside the range of our study. The bands at 3312 and 3236 cm^{-1} are assigned to the ν_3 and ν_1 OH stretching bands, respectively, and the 1696 cm^{-1} band is assigned to the OH bending mode of the hydrogen-bonded water molecules. In Figure 3, spectrum c of the dehydrated CaGlBPD shows, as expected, a major intensity reduction in these bands; in addition, the bands at 746 and 698 cm^{-1} are absent. The 746 and 698 cm^{-1} bands are assigned to librational modes of the water molecules. One of the three librational modes (twisting-type mode) is expected to have weak infrared intensity[27] and may have escaped detection. The number of observed bands for each H_2O mode, two stretching bands, one bending band, and two of the three librational bands, is consistent with all H_2O molecules occupying equivalent sites in the crystals which agrees with the X-ray structure result. The absence of additional bands for the four detected modes, under the resolution used (2 cm^{-1}), indicates coupling between the H_2O modes does not occur.

Powder X-ray Diffraction. The PXRD results (Table 3) show good agreement between the calculated *d* spacing values obtained from the single-crystal data and the observed *d* spacing values obtained from the X-ray powder diffraction pattern. The overall agreement between the powder data and the crystal structure data attests to the validity of both data.

Crystal Structure. The α-keto group to the phosphonate is expected to form chelate bonds to metal ions; this is supported by only one structure determination for monosodium acetylphosphonate with a partially ionized PO_3H group.[13] Chelate complexes of diethyl acetylphosphonate with transition metal ions have been characterized by infrared and electronic spectra.[28] However, this cannot be considered as a true keto phosphonate since two of the three O atoms are esterified and, therefore, not available for metal ion bonding. This study provides the first confirmation of such a chelate bond involving an α-keto group and a completely ionized phosphonate group with a Ca ion.

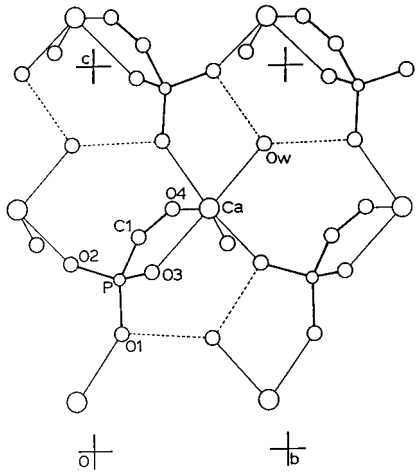

Figure 6. View down the *b*-axis of a single sheet of calcium phosphonate layer showing the environment around Ca and phosphonate group.

Phosphonates can be considered as hybrid organic/inorganic materials that can be related to those of inorganic phosphates. For example, zirconium phosphonate, $Zr(O_3PR)_2$, can be considered a structural derivative of layered α-$Zr(HPO_4)_2{\cdot}H_2O$[29] with the organic group substituting for the OH group.[30−32] In both compounds, Zr has an octahedral coordination, each O atom of the PO_3 group is bonded to a different Zr atom, and the area of coverage per PO_3 group is 24 $Å^2$ (Figure 7a). Recent studies have shown similar layer-type arrangement in several divalent metal phosphonates.[31−37] The phosphonate groups are bonded to a central layer of metal atoms from either side forming an inorganic layer. The detailed atomic arrangement in this layer depends on the bonding requirements of the metal atoms and the ionization of the phosphonate group with little influence of the organic portion. In the case of the monophosphonates, the bonding between layers consists of van der Waals contacts between the end groups of alkyl or aryl chains of adjacent layers. Dines et al.[38] were the first to propose and prepare pillared or cross linked compounds by using bis(phosphonic acid) where the terminal PO_3 are covalently linked. Recent structural studies have shown that the layer-type arrangement and the metal phosphonate linkage in the bis(phosphonates) are strikingly similar to those of the corresponding monophosphonates.[39,40]

(22) Sverdlov, L. M.; Kovner, M. A.; Krainov, E. P. *Vibrational Spectra of Polyatomic Molecules*; Wiley: New York, 1974; Chapter III.
(23) Suzuki, M.; Shimanouchi, T. *J. Mol. Spectrosc.* **1969**, *29*, 415.
(24) Ferraro, J. R.; Ziomek, J. S. *Introductory Group Theory and its Application to Molecular Structure*; Plenum Press: New York, 1975; p 23.
(25) Raghuvanshi, G. S.; Khandelwal, D. P.; Bist, H. D. *Appl. Spectrosc.* **1984**, *38* (5), 710.
(26) Falk, M.; Knop, O. In *Water: A Comprehensive Treatise, Vol 2: Water in Crystalline Hydrates; Aqueous Solutions of Simple Nonelectrolytes*; Franks, F., Ed.; Plenum Press: NewYork, 1973; Chapter 2.
(27) Miyazawa, T. *Bull. Chem. Soc. Jpn.* **1961**, *34*, 202.
(28) Mikulski, C. M.; Henry, W.; Pytlewski, L. L.; Karayannis, N. M. *J. Inorg. Nucl. Chem.* **1978**, *40*, 769.
(29) Clearfield, A.; Smith, G. D. *Inorg. Chem.* **1969**, *8*, 431.
(30) Dines, M. B.; DiGiacomo, P. *Inorg. Chem.* **1981**, *20*, 92.
(31) Cao, G.; Hong, H.; Mallouk, T. E. *Acc. Chem. Res.* **1992**, *25*, 420.
(32) Thompson, M. E. *Chem. Mater.* **1994**, *6*, 1168.
(33) Cao, G.; Lynch, V. M.; Swinnea, J. S.; Mallouk, T. E. *Inorg. Chem.* **1990**, *29*, 2112.
(34) Cao, G.; Lee, H.; Lynch, V. M.; Mallouk, T. E. *Solid State Ionics* **1988**, *26*, 63.
(35) Cao, G.; Lee, H.; Lynch, V. M.; Mallouk, T. E. *Inorg. Chem.* **1988**, *27*, 2781.
(36) Martin, K. J.; Squattrito, P. J.; Clearfield, A. *Inorg. Chim. Acta* **1989**, *155*, 7.
(37) Cao, G.; Lee, H.; Lynch, V. M.; Yacullo, L. N. *Chem. Mater.* **1993**, *5*, 1000.
(38) Dines, M. B.; Cooksey, R. E.; Griffith, P. C.; Lane, R. H. *Inorg. Chem.* **1983**, *22*, 1003.
(39) Poojary, D. M.; Zhang, B.; Bellinghausen, P.; Clearfield, A. *Inorg. Chem.* **1996**, *35*, 4942.
(40) Poojary, D. M.; Zhang, B.; Bellinghausen, P.; Clearfield, A. *Inorg. Chem.* **1996**, *35*, 5254.

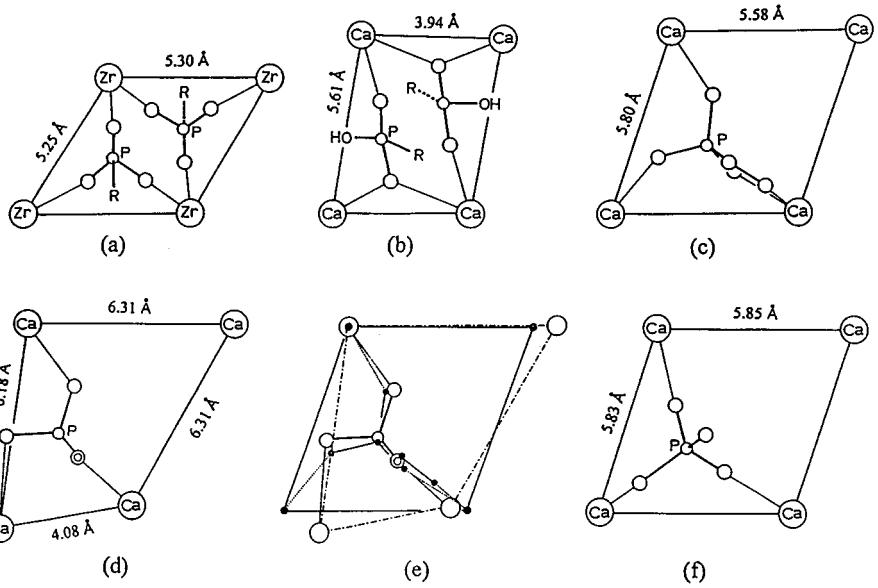

Figure 7. Comparison of metal−phosphonate interactions with Ca−phosphate interactions in OHAp. The area (*A*) of the metal ion quadrilateral is given. Key: (a) $Zr(O_3PR)_2$ and α-$ZrHPO_4$ when R = OH, $A = 24.0$ Å^2; (b) $Ca(HO_3PC_6H_{13})_2$, $A = 20.8$ Å^2; (c) (010) face of CaGlBPD, $A = 30.6$ Å^2; (d) the (001) face of OHAp, $A = 29.3$ Å^2; (e) the superposition of the (001) face of OHAp on the (010) face of CaGlBPD [(d) superimposed on (c). The contents of only one Ca ion quadrilateral are considered. The open circles represent atomic positions in OHAp, while the filled circles represent those in CaGlBPD]; (f) the (100) face of OHAp. Only the ions in a section at $x \sim 0$ are considered. $A = 32.5$ Å^2.

The general structural features of the calcium monophosphonates,[33] $Ca(HO_3PC_6H_{13})_2$ and $Ca(O_3PCH_3)\cdot H_2O$, are similar to those of α-$Zr(HPO_4)_2\cdot H_2O$ and $Zr(O_3PR)_2$. The Ca atom in $Ca(HO_3PC_6H_{13})_2$ has an octahedral coordination and a metal phosphonate coordination ratio 6:3 as in $Zr(O_3PR)_2$. However, since the OH group is noncoordinating to Ca, one of the oxygen atoms of the phosphonate group is bridging two Ca atoms (Figure 7b). The basal area per phosphonate group is only 20.8 Å^2. $Ca(O_3PCH_3)\cdot H_2O$ also has a layered structure similar to $Ca(HO_3PC_6H_{13})_2$.[33] $Ca(O_3PCH_3)\cdot H_2O$ has a completely ionized PO_3 and, therefore, is chemically similar to CaGlBPD. The Ca plane in $Ca(O_3PCH_3)\cdot H_2O$ is rather puckered, and the coordination of the Ca atom consists of a distorted octahedron. Three phosphonate oxygen atoms are bonded to a total of five Ca atoms, with two Ca bridging bonds. The metal phosphonate coordination ratio is 5:5 with the sixth coordination site occupied by a water molecule. In several metal phosphonates of the formula $M(O_3PR)\cdot H_2O$, for M = Mg, Mn, Zn, and Cd, the phosphonate group is involved in a bidentate chelate bond to the metal ion.[34−37]

Although the general features of Ca−PO_3 linkage in CaGlBPD are similar to those in Ca monophosphonates and α-$Zr(HPO_4)_2\cdot H_2O$, major deviations imposed by the chelating keto group can be clearly seen (Figure 7c). In Ca monophosphonates and α-$Zr(HPO_4)_2\cdot H_2O$, the octahedral coordination is attained by sets of triangular O atoms above and below the plane of the central metal atom. In CaGlBPD, the coordinating O atoms of the PO_3 group are nearly in the plane of the Ca ions; these O atoms and the water molecule occupy the equatorial plane of the Ca octahedron, with the chelating keto group in one of the axial positions. To accommodate the phosphonate O atoms approximately in the plane of the Ca ions, the Ca positions are enlarged, so that, in effect, the basal area of coverage per phosphonate group can be considered to have increased to 30.6 Å^2. Although the phosphonate group is bonded to only three of the Ca positions in the parallelogram, the fourth Ca site is linked to the PO_3 group through strong hydrogen bonding from the water molecule at this Ca site. The increased area of coverage per phosphonate group and the stabilization of this structural feature can be attributed to the chelate bond involving the keto group. The electron-withdrawing nature of the keto group plays the vital role in producing a completely ionized BP at neutral pH to facilitate this structure. Un-ionized phosphonate O atoms are not known to bind to the metal ions in monophosphonate structures[33] or geminal bis(phosphonates).[11,12]

Comparison of the structures of hydroxyapatite,[41] $Ca_5(PO_4)_3$-OH (OHAp), and CaGlBPD can be used to derive possible models of interaction of bis(acylphosphonate) ions in controlling Ca-related disorders. OHAp is the structural prototype of the major constituent of tooth, bone, and calcified deposits. One of the most interesting consequences of the expanded Ca ion positions in the (010) face of CaGlBPD is that the distribution of Ca in these layers is closely related to those of the Ca ions on the most prominent faces, (001) and (100), of OHAp (Figure 7).

A projection of the structure of OHAp[41] along (001), a section at $z = {}^1/_4$, is shown in Figure 8. All the Ca and the phosphate ions shown are on the mirror plane at $z = {}^1/_4$, except for the column calcium, Ca1 (which is at $z = 0$ or ${}^1/_2$). This arrangement is very similar to the Ca phosphonate layer in CaGlBPD which also has all the Ca ions exactly planar. If we consider the triangular Ca positions in OHAp (around Ca1 in Figure 8), they match very closely to that of the triangle of Ca ions linked by the same BP ion (Figure 6). The positions of the three O atoms around the Ca1 also matches closely to that of the phosphonate O atoms in CaGlBPD. A closer similarity can be seen if we consider the phosphonate group displacing the PO_4 group. While O1 and O2 are linked to two Ca ions in unidentate fashion in both OHAp and CaGlBPD, the O3−O4 chelate bond in CaGlBPD mimics the O3−O3′ (related by mirror symmetry at $z = {}^1/_4$) chelate bond in OHAp (Figure 7). Thus, there is a nearly perfect lattice match of the Ca ions and the phosphate/phosphonate ions allow optimal binding of the incoming acylphosphonate group of the inhibitor. The effective area of coverage per phosphate group may be considered as the area

(41) Kay, M. I.; Young, R. A.; Posner, A. S. *Nature (London)* **1964**, *204*, 1050.

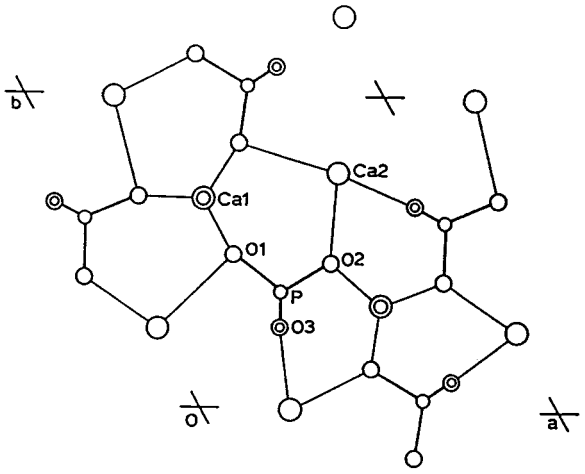

Figure 8. Structure of OHAp, projected along (001). Only the atoms in the plane at $z = {}^1/_4$ are shown, except for Ca1 and O3 which occupy positions related by the mirror plane at $z = {}^1/_4$.

of the Ca quadrilateral, which is 29.3 Å^2 in good agreement with the value found for the phosphonate group in CaGlBPD. The (100) face of OHAp also has a plane of Ca ions with similar Ca−Ca distances as in the (010) face of CaGlBPD indicating they also can function as a probable site for binding of BP (Figure 7f).

The structural features and the lattice matching observed in these studies can be used to derive a simple model for the physicochemical interaction of the acyl BP with OHAp crystal surfaces. The unique structural match observed in CaGlBPD and OHAp crystal surfaces indicates that they are prime candidates for possible epitaxial growth on one another. Epitaxial mechanisms have been proposed to play major roles in controlling the nucleation and crystal growth of phases associated with many biomineralization processes.[42] However, surface adsorption mechanisms are often implicated in preference to epitaxy since it is only necessary to have a relatively small percent of the surface area covered by the adsorbed material for complete inhibition of growth.[43] In either case, geometric and stereochemical matching are key factors. A possible simple mechanism is that the phosphonate or the calcium phosphonate complex can selectively block active growth sites on the surface of OHAp, thus slowing down the crystal growth rate. Each phosphonate ion in the present study is bonded to three different Ca ions which would result in more effective blocking of active sites. The fact that the {100} and {001} faces account for almost the entire surface of apatite crystals supports the effectiveness of this BP in controlling the growth of OHAp.

The lack of biological activity of the long-chain bis(phosphonates) devoid of any ortho functional group can be related to its inability to emulate the structural match observed here. However, the lattice match observed here cannot alone account for the biological activity of these bis(phosphonates). Although similar Ca−phosphonate interactions and lattice matches can be expected of monoacylphosphonates, they possess much lower biological activity.[9,10] This lends additional support to the synergic effects of bis(phosphonate) groups. Since the two acylphosphonate groups in the GlBP ion are connected by a rigid hydrocarbon chain and independently bonded to different sets of Ca ions, they are capable of binding simultaneously to two different active sites or faces on two different OHAp crystals. Consequently, the GlBP ion is a more efficient inhibitor than any molecule with a single functional group.

Recent studies of the effects of bis(phosphonates) on the crystallization of barite (barium sulfate) indicate other modes of interaction. Experimental evidence shows that bis(phosphonates) are actually incorporated into the barite surface lattice rather than just adsorbed onto the surface.[44,45] Another interesting observation was that calcium phosphonate complexes were the active inhibitors.[46] The mechanism proposed consists of a replacement of two nearest-neighbor sulfate ions (with S−S separation of 5.6 Å) by a bis(phosphonate) ion (with P−P separation of 5.7 Å) on the (011) crystal surface. Although molecular modeling studies are in general agreement with this configuration for the (011) face, prediction that the bis(phosphonate) ion will enter the (100) face also was not experimentally verified.[47] However, this model is limited to bis(phosphonates) separated by a three-atom chain to have a P−P separation of 5.7 Å. Moreover, on the basis of the general structural features of metal−phosphonate interactions, the nongeminal bis(phosphonates) would be expected to interact with two different faces perpendicular to the alkyl chain rather than embed into a single face of a crystal.

Although inhibitors are generally considered to act by the classical mechanism of blocking crystal growth sites, they may also act as nucleation promoters. In many biomineralizing systems, organized organic assemblies serve as inductive templates for mediating the nucleation and growth of inorganic crystals. Recently, the application of highly organized two-dimensional surfaces, such as Langmuir monolayers, as potential templates for regulating the nucleation and growth of inorganic crystals have been studied.[48−50] These studies have shown that the oriented nucleation of crystals can be achieved when the two-dimensional domains of the monolayer are structurally compatible with the two-dimensional lattice of the specific crystal phases. The nucleation and growth of barium sulfate can be controlled by compressed Langmuir monolayers of aliphatic long-chain phosphonates, although the alkylphosphonates are themselves known to be potent inhibitors of crystal growth.[50] The two-dimensional phosphonate layer observed in CaGlBPD can be considered similar to that of the phosphonate layer in the Langmuir monolayer. The lattice match observed between the Ca phosphonate layer in CaGlBPD and the OHAp faces indicates that the Ca phosphonate layer could act as possible sites for the oriented nucleation and crystal growth of OHAp.

Acknowledgment. This investigation was supported, in part, by USPHS Research Grant DE05030 (M.M.) and HL30035 (N.E) to the American Dental Association Health Foundation

(42) Addadi, L.; Weiner, S. In *Biomineralization: Chemical and Biochemical Perspectives*; Mann, S., Webb, J., Williams, R. J. P., Eds; VCH Press: Weinheim, Germany, 1989; p 133.
(43) Leung, H.; Nancollas, G. H. *J. Cryst. Growth* **1978**, *44*, 163.
(44) Davey, R. J.; Black, S. N.; Broomley, L. A.; Cottier, D.; Dobbs, B.; Rout, J. E. *Nature* **1991**, *353*, 549.
(45) Black, S. N.; Broomley, L. A.; Cottier, D.; Davey, R. J.; Dobbs, B.; Rout, J. E. *J. Chem. Soc., Faraday Trans.* **1991**, *87*, 3409.
(46) Benton, W. J.; Collins, I. R.; Grimsey, I. M.; Parkinson, G. M.; Rodger, S. A. *Faraday Discuss.* **1993**, *95*, 281.
(47) Rohl, A. L.; Gay, D. H.; Davey, R. J.; Catlow, C. R. A. *J. Am. Chem. Soc.* **1996**, *118*, 642.
(48) Rajam, S.; Heywood, B. R.; Walker, J. B. A.; Mann, S.; Davey, R. J.; Birchall, J. D. *J. Chem. Soc., Faraday Trans.* **1991**, *87*, 727.
(49) Heywood, B. R.; Mann, S. *J. Am. Chem. Soc.* **1992**, *114*, 4681.
(50) Heywood, B. R.; Mann, S. *Langmuir* **1992**, *8*, 1492.
(51) Certain commercial materials and equipment are identified in this paper to specify the experimental procedure. In no instance does such identification imply recommendation or endorsement by the National Institute of Standards and Technology or the ADA Health Foundation or that the material or equipment identified is necessarily the best available for the purpose.

from the National Institutes of Health and is part of the dental research program conducted by the National Institute of Standards and Technology in cooperation with the American Dental Association Health Foundation. It was also supported, in part, by the German Israeli Foundation for Scientific Research and Development (to E.B. and G.G.). E.B. and G.G. are affiliated with the David R. Bloom center for pharmacy. The authors thank Dr. B. J. Bauer, Polymers Division, NIST, for the TG measurement.

Supporting Information Available: Tables of crystallographic and refinement data and anisotropic thermal parameters (2 pages). Ordering information is given on any current masthead page.

IC980374H